Articles

Synthesis and Solid State Structures of Functionalized Phenyleneethynylene Trimers in 2D and 3D

Paolo Samorí,[†,§] Viola Francke,[‡] Volker Enkelmann,[‡] Klaus Müllen,*[,‡] and Jürgen P. Rabe*[,†]

Department of Physics, Humboldt University Berlin, 10099 Berlin, Germany, and Max-Planck-Institute for Polymer Research, Postfach 3148, 55021 Mainz, Germany

Received June 25, 2002. Revised Manuscript Received September 19, 2002

Novel soluble end-functionalized phenyleneethynylene oligomers were synthesized via efficient Pd-catalyzed coupling. The structures, both of single crystals and of monolayers at the solid−liquid interface, were resolved respectively by means of X-ray diffraction (XRD) and scanning tunneling microscopy (STM) at submolecular resolution. They revealed either 3D or 2D highly ordered architectures consisting of rodlike π-conjugated skeletons and flexible hexyl side chains which possess a considerable conformational mobility at room temperature. The self-assembly arises from the cooperative effect of intermolecular and intramolecular interactions among the unsaturated backbone, the hexyl side chains, the hydrophilic end groups, and eventually the substrate as discussed in detail. Finally, the STM investigation made it possible to monitor molecular-scale defects in the polycrystals.

1. Introduction

Organic semiconducting materials, such as π-conjugated oligomers and polymers, possess unique electronic properties which open a wide range of applications both in optoelectronics and photonics.[1] A fine-tuning of the performance of molecular-based devices depends on the spatial arrangement of the molecules. Therefore, it is a fundamental goal to drive the molecular self-assembly on flat solid substrates toward highly ordered, reproducible, and thermodynamically stable supramolecular structures. In this context, due to their easier processability, oligomers are commonly investigated as model compounds of their related macromolecules.[2] In particular, oligothiophenes have gained considerable interest[1b,3] for their electro-optical properties,[4] but also *p*-phenyleneethynylene derivatives have received attention:[5] besides their interesting optoelectronic properties,[6] they exhibit a remarkable stiffness and linearity along the conjugated backbone[7] that allow them to self-assemble into well-defined nanostructures[8−10] and make

* To whom correspondence should be addressed. E-mail: muellen@mpip-mainz.mpg.de; rabe@physik.hu-berlin.de.
† Humboldt University Berlin.
‡ Max-Planck-Institute for Polymer Research.
§ New address: Istituto per la Sintesi Organica e la Fotoreattività, C.N.R. Bologna, via Gobetti 101, 40129 Bologna, Italy.

(1) (a) Burroughes, J. H.; Bradley, D. D. C.; Brown, A. R.; Marks, R. N.; Mackay, K.; Friend, R. H.; Burns, P. L.; Holmes, A. B. *Nature* **1990**, *347*, 539. (b) Garnier, F.; Hajlaoui, R.; Yassa, A.; Srivastava, P. *Science* **1994**, 265, 1684. (c) Yu, G.; Gao, J.; Hummelen, J. C.; Wudl, F.; Heeger, A. J. *Science* **1995**, *270*, 1789. (d) Stabel, A.; Herwig, P.; Müllen, K.; Rabe, J. P. *Angew. Chem., Int. Ed. Engl.* **1995**, *34*, 1609. (e) Lidzey, D. G.; Bradley, D. D. C.; Alvarado, S. F.; Seidler, P. F. *Nature* **1997**, *386*, 135. (f) Friend, R. H.; Gymer, R. W.; Holmes, A. B.; Burroughes, J. H.; Marks, R. N.; Taliani, C.; Bradley, D. D. C.; Dos Santos, D. A.; Brédas, J. L.; Lögdlund, M.; Salaneck, W. R. *Nature* **1999**, *397*, 121. (g) Cacialli, F.; Wilson, J. S.; Michels, J. J.; Daniel, C.; Silva, C.; Friend, R. H.; Severin, N.; Samorí, P.; Rabe, J. P.; O'Connell, M. J.; Taylor, P. N.; Anderson, H. L. *Nature Materials* **2002**, *1*, 160.
(2) Müllen, K.; Wegner, G. *Electronic Materials: The Oligomer Approach*; Wiley−VCH: Weinheim, Germany, 1998.
(3) (a) Biscarini, F.; Zamboni, R.; Samorí, P.; Ostoja, P.; Taliani, C. *Phys. Rev. B* **1995**, *52*, 14868. (b) Bäuerle, P.; Fischer, T.; Bidlingmeier, B.; Stabel, A.; Rabe, J. P. *Angew. Chem., Int. Ed. Engl.* **1995**, *34*, 303. (c) Gesquière, A.; Abdel-Mottaleb, M. M. S.; De Feyter, S.; De Schryver, F. C.; Schoonbeek, F.; van Esch, J.; Kellogg, R. M.; Feringa, B. L.; Calderone, A.; Lazzaroni, R.; Brédas, J. L. *Langmuir* **2000**, *16*, 10385.
(4) (a) Ziegler, Ch. In *Handbook of organic conductive molecules and polymers*; Nalwa, H. S., Ed.; John Wiley & Sons: New York, 1997. (b) Bolognesi, A.; Bajo, G.; Paloheimo, J.; Ostergard, T.; Stubb, H. *Adv. Mater.* **1997**, *9*, 121. (c) Taliani, C.; Biscarini, F.; Muccini M. In *Seminconducting Polymers−Chemistry, Physics and Engineering*; Hadzioannou, G., van Hutten, P. F., Eds.; Wiley−VCH: Weinheim, Germany, 1999. (d) Barbarella, G.; Favaretto, L.; Sotgiu, G.; Zambianchi, M.; Fattori, V.; Cocchi, M.; Cacialli, F.; Gigli, G.; Cingolani, R. *Adv. Mater.* **1999**, *11*, 1375.
(5) (a) Kondo, K.; Okuda, M.; Fujitani, T. *Macromolecules* **1993**, *26*, 7382. (b) Tour, J. M. *Chem. Rev.* **1996**, *96*, 537. (c) Giesa, R. *J. Macromol. Sci Rev. Chem. Phys.* **1996**, *C36*, 631. (d) Bunz, U. H. F. *Chem. Rev.* **2000**, *100*, 1605.
(6) (a) Weder, C.; Wrighton, M. S. *Macromolecules* **1996**, *29*, 5157. (b) Weder, C.; Sarwa, C.; Montali, A.; Bastiaansen, C.; Smith, P. *Science* **1998**, *279*, 835. (c) Montali, A.; Bastiaansen, C.; Smith, P.; Weder, C. *Nature* **1998**, *392*, 261. (d) Levitsky, I. A.; Kim, J.; Swager, T. M. *J. Am. Chem. Soc.* **1999**, *121*, 1466.
(7) (a) Moroni, M.; Le Moigne, J.; Luzzati, S. *Macromolecules* **1994**, *27*, 562. (b) Wautelet, P.; Moroni, M.; Oswald, L.; Le Moigne, J.; Pham, A.; Bigot, J. Y.; Luzzati, S. *Macromolecules* **1996**, *29*, 446. (c) Moroni, M.; Le Moigne, J.; Pham, A.; Bigot, J. Y. *Macromolecules* **1997**, *30*, 1964.
(8) (a) Kim, J.; McHugh, S. K.; Swager, T. M. *Macromolecules* **1999**, *32*, 1500. (b) Samorí, P.; Francke, V.; Müllen, K.; Rabe, J. P. *Chem. Eur. J.* **1999**, *5*, 2312. (c) Samorí, P.; Severin, N.; Müllen, K.; Rabe, J. P. *Adv. Mater.* **2000**, *12*, 579. (d) McQuade, D. T.; Kim, J.; Swager, T. M. *J. Am. Chem. Soc.* **2000**, *122*, 5885. (e) Steffen, W.; Bunz, U. H. F. *Macromolecules* **2000**, *33*, 9518. (f) Kim, J.; Swager, T. M. *Nature* **2001**, *411*, 1030.
(9) (a) Li, H.; Powell, D. R.; Hayashi, R. K.; West, R. *Macromolecules* **1998**, *31*, 52. (b) Bunz, U. H. F.; Enkelmann, V.; Kloppenburg, L.; Jones, D.; Shimizu, K. D.; Claridge, J. B.; zur Loye, H.-C.; Lieser, G. *Chem. Mater.* **1999**, *11*, 1416.

10.1021/cm0212459 CCC: $25.00
Published on Web 11/16/2002

them candidates for molecular nanowires in molecular-scale electronic devices.[11]

We report here on the synthesis and characterization of the thiol end-functionalized phenyleneethynylene trimer, namely, α-[[4-[(*N*,*N*-dimethylcarbamoyl)thio]-phenyl]ethynyl]-*ω*-[4-[(*N*,*N*-dimethylcarbamoyl)thio]phenyl]-ter[(2,5-dihexylphenylene-1,4)ethynylene)] (**1**) and of the phenyl functionalized one, α-phenylethynyl-*ω*-phenyl-ter [(2,5-dihexylphenylene-1,4)ethynylene)] (**2**). These soluble oligomers serve as model compounds for the α,*ω*-thiol functionalized poly(*p*-phenyleneethynylene)s.[8b,12] Their structures have been defined by means of X-ray diffraction (XRD) on the single crystal and scanning tunneling microscopy (STM) at the solid−liquid interface. STM imaging allowed us also to visualize molecular-scale defects in the crystal lattice. Furthermore, the structure of a single crystal of 1,4-bis[2-[4-[(*N*,*N*-dimethylcarbamoyl)thio]phenyl]ethynyl-2,5-dihexylbenzene (**9**) has been resolved as a model system for comparison.

2. Results and Discussion

2.1. Synthesis. α-[[4-[(*N*,*N*-Dimethylcarbamoyl)thio]-phenyl]ethynyl]-*ω*-[4-[(*N*,*N*-dimethylcarbamoyl)thio]phenyl]-ter[(2,5-dihexylphenylene-1,4)ethynylene)] (**1**) and α-phenylethynyl-*ω*-phenyl-ter[(2,5-dihexylphenylene-1,4)ethynylene)] (**2**) were synthesized by Pd-catalyzed coupling (Scheme 1).[12,13] The first step toward the end-functionalized trimers **1** and **2** was the synthesis of 1,4-bis[[2,5-dihexyl-4-(trimethylsilylethynyl)phenyl]ethynyl]-2,5-dihexylbenzene (**5**) by coupling of 2,5-dihexyl-4-[(trimethylsilyl)ethynyl]iodobenzene (**3**)[12] with 1,4-diethynyl-2,5-dihexylbenzene[14] (**4**) under $Pd(PPh_3)_4$/CuI catalysis (Scheme 1). After removal of the trimethylsilyl groups, the resulting 1,4-bis[(4-ethynyl-2,5-dihexylphenyl)ethynyl]-2,5-dihexylbenzene (**6**) was reacted either with the end-capping reagent 4-[(*N*,*N*-dimethylcarbamoyl)thio]iodobenzene (**7**)[12] or with iodobenzene to yield, respectively, **1** or **2**.

Furthermore, 1,4-bis[2-[4-[(*N*,*N*-dimethylcarbamoyl)-thio]phenyl]ethynyl-2,5-dihexylbenzene (**9**) was also synthesized by Pd-catalyzed coupling of 1,4-diethynyl-2,5-dihexylbenzene (**4**) with the end-capping reagent 4-[(*N*,*N*-dimethylcarbamoyl)thio]iodobenzene (**7**) under Hagihara conditions (Scheme 2).

2.2. STM Investigation. A monodisperse molecular system can physisorb at the interface between its almost saturated solution and a highly oriented pyrolytic graphite (HOPG) substrate in a polycrystalline monolayer where the orientation of each single crystallite is determined by the 3-fold symmetry of the support.[1d,3b,c,8b,c,15] The structure of a single crystallite of **1**

Scheme 1. Synthesis of α-[[4-[(*N*,*N*-Dimethylcarbamoyl)thio]phenyl]-ethynyl]-*ω*-[4-[(*N*,*N*-dimethylcarbamoyl)thio]-phenyl]-ter[(2,5-dihexylphenylene-1,4)ethynylene)] (1) and α-Phenylethynyl-*ω*-phenyl-ter[(2,5-dihexylphenylene-1,4)ethynylene)] (2)

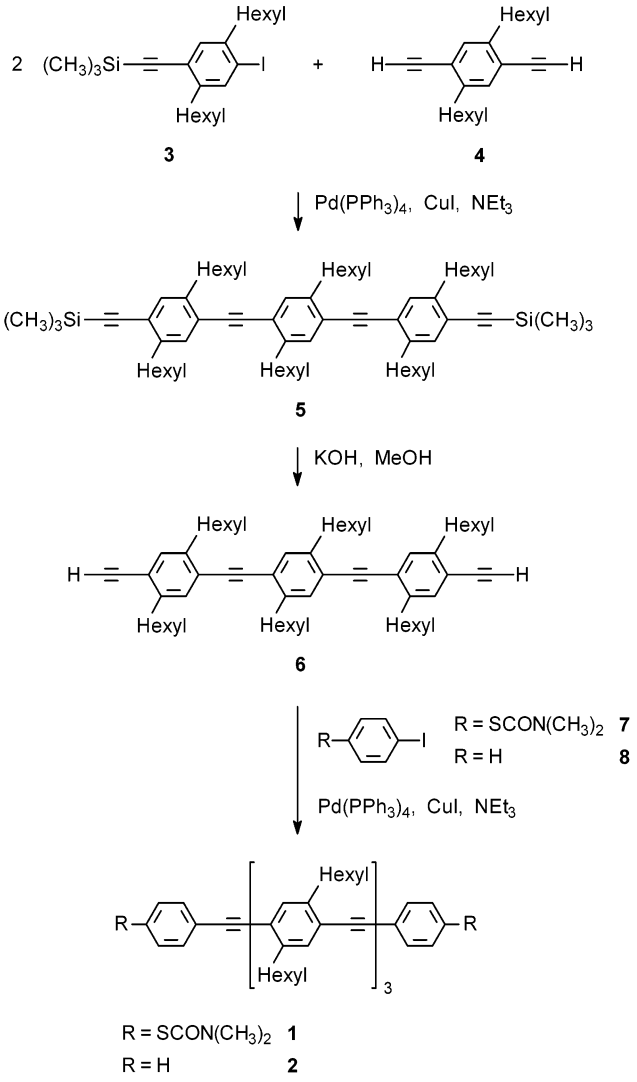

Scheme 2. Synthesis of 1,4-Bis[2-[4-[(*N*,*N*-dimethylcarbamoyl)thio]phenyl]-ethynyl-2,5-dihexylbenzene (9)

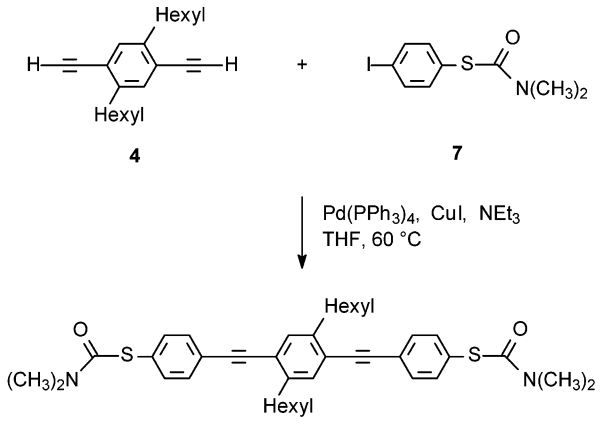

(10) Leclère, Ph.; Calderone, A.; Marsitzky, D.; Francke, V.; Geerts, Z.; Müllen, K.; Brédas, J. L.; Lazzaroni, R. *Adv. Mater.* **2000**, *12*, 1042.

(11) (a) Bumm, L. A.; Arnold, J. J.; Cygan, M. T.; Dunbar, T. D.; Burgin, T. P.; Jones II, L.; Allara, D. L.; Tour, J. M.; Weiss, P. S. *Science* **1996**, *271*, 1705. (b) Dhirani, A.; Zehner, R. W.; Hsung, R. P.; Guyot-Sionnest, P.; Sita, L. R. *J. Am. Chem. Soc.* **1996**, *118*, 3319. (c) Dhirani, A.; Lin, P.-H.; Guyot-Sionnest, P.; Zehner, R. W.; Sita, L. R. *J. Chem. Phys.* **1997**, *106*, 5249. (d) Cygan, M. T.; Dunbar, T. D.; Arnold, J. J.; Bumm, L. A.; Shedlock, N. F.; Burgin, T. P.; Jones, L., II; Allara, D. L.; Tour, J. M.; Weiss, P. S. *J. Am. Chem. Soc.* **1998**, *120*, 2721.

(12) Francke, V.; Mangel, T.; Müllen, K. *Macromolecules* **1998**, *31*, 2447.

(13) (a) Dieck, H. A.; Heck, R. F. *J. Organomet. Chem.* **1975**, *93*, 259. (b) Cassar, L. *J. Organomet. Chem.* **1975**, *93*, 253. (c) Sonogashira, K.; Tohda, Y.; Hagihara, N. *Tetrahedron Lett.* **1975**, 4467.

(14) Mangel, T.; Eberhardt, A.; Scherf, U.; Bunz, U. H. F.; Müllen, K. *Macromol. Rapid Commun.* **1995**, *16*, 571.

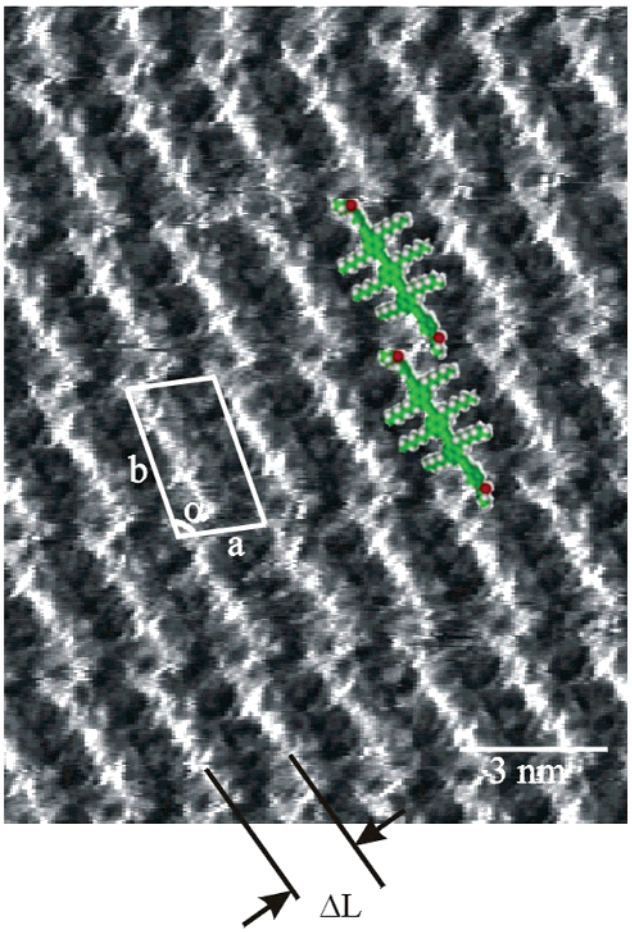

Figure 1. STM image recorded in constant height mode of **1** at the HOPG−solution interface. Tip bias (U_t) = 1.2 V, average tunneling current (I_t) = 1.0 nA. 2-D crystal structure with a unit cell: $a = 1.83 \pm 0.11$ nm, $b = 3.42 \pm 0.12$ nm, $\alpha = 108 \pm 5°$. The distance between adjacent parallel backbones is $\Delta L = 1.52 \pm 0.08$ nm. The angles between the backbone and the lamella main direction amounts to $67 \pm 2°$.

is displayed in Figure 1. Both the aliphatic side chains and the conjugated skeletons lie flat on the (0001) plane of graphite. Since the contrast in STM constant height mode imaging is mainly determined by the energy difference between the electronic states of the adsorbate and the Fermi level of the substrate, darker parts can be ascribed to the aliphatic groups, characterized by a larger energy difference, and bright rods can be assigned to the backbones.[16]

The spacing between consecutive parallel backbones (ΔL) in Figure 1 amounts to 1.52 ± 0.08 nm. This is considerably smaller than the width of the molecules calculated for the case with the hexyl chains extended, which amounts to 1.9 nm. It indicates that the side chains are disordered between adjacent parallel backbones since an interdigitation of these groups can be excluded due to steric hindrance. This disordered conformation corresponds to a high mobility of the alkyl substituents at room temperature, which takes place on a time scale faster than the scanning frequency; consequently, it was not possible to resolve their structures. In the present case the formation of tightly packed crystals epitaxially grown on the basal plane of the substrate seems to be favored by the high stiffness of the backbone, which is composed of alternating phenylene and ethynylene groups. A slight interdigitation of the carbamoyl end groups in the 2D pattern can be recognized. It is likely to be induced by hydrogen bondings between neighboring carbamoyl groups. This not only stabilizes the crystal structure but also impedes a columnar packing which was found for mixtures of alkane monolayers crystallized on the basal plane of HOPG.[17]

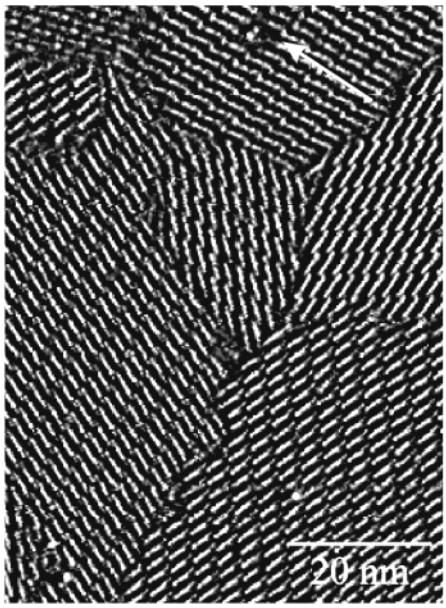

Figure 2. STM image in constant height mode of **1** at the solid−liquid interface. $U_t = 1.2$ V, average $I_t = 1.0$ nA. Polycrystalline structure made of domains with different molecular orientations. The arrow indicates a defect (two missing molecules) in the crystal lattice.

On a larger scale a monolayer of **1** is polycrystalline (see Figure 2). The orientation of the molecules in each single crystallite is symmetry-equivalent with respect to the crystalline substrate. The high-resolution imaging achieved in the polycrystalline structure made it possible to record two different kinds of defects on the nanometer and the sub-nanometer length scale. A first kind of defects are missing molecules within a single molecular crystallite; an example of two missing molecules is indicated by an arrow in Figure 2. A second kind of defects are the domain boundaries that surround each crystal. At these frontiers the molecules are more loosely packed. A notably high dynamics of the molecules at the solid−liquid interface, within the time scale of the STM imaging, has been monitored not only at the domain boundaries (leading eventually to 2D-Ostwald ripening[18]) but also within the crystals, namely, where a missing-molecule defect is located. This dynam-

(15) (a) Rabe, J. P.; Buchholz, S. *Phys. Rev. Lett.* **1991**, *66*, 2096. (b) Rabe, J. P.; Buchholz, S. *Science* **1991**, *253*, 424. (c) Cyr, D. M.; Venkataraman, B.; Flynn, G. W.; Black, A.; Whitesides, G. M. *J. Phys. Chem.* **1996**, *100*, 13747. (d) Claypool, Ch. L.; Faglioni, F.; Goddard, W. A., III.; Gray, H. B.; Lewis, N. S.; Marcus, R. A. *J. Phys. Chem. B* **1997**, *101*, 5978. (e) Strawasz, M. E.; Sampson, D. L.; Parkinson, B. A. *Langmuir* **2000**, *16*, 2326.

(16) Lazzaroni, R.; Calderone, A.; Brédas, J. L.; Rabe, J. P. *J. Chem. Phys.* **1997**, *107*, 99.

(17) Hentschke, R.; Askadskaya, L.; Rabe, J. P. *J. Chem. Phys.* **1992**, *97*, 6901.

(18) Stabel, A.; Heinz, R.; De Schryver, F. C.; Rabe, J. P. *J. Phys. Chem.* **1995**, *99*, 505.

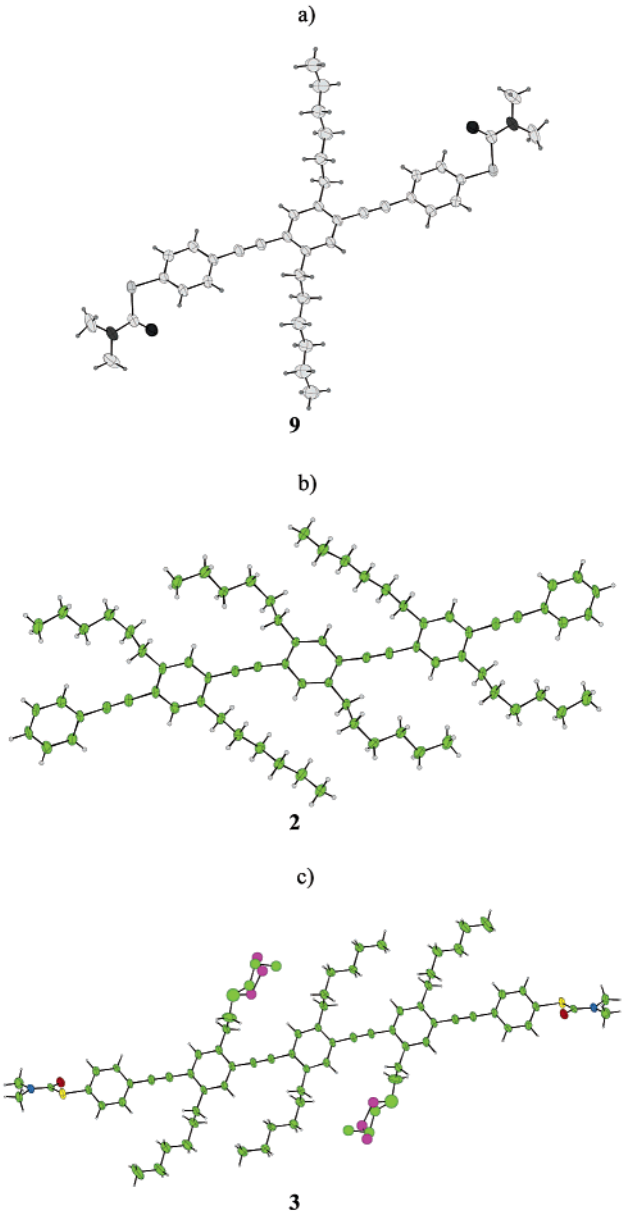

Figure 3. Single molecular structure in single crystals of (a) **9**, (b) **2**, and (c) **1**.

ics allowed to recover in a few minutes the defect of the first type shown in Figure 2.

2.3. XRD Characterization. The single-crystal structures of the **1**, **2**, and **9** were determined by means of XRD. ORTEP plots (fORtran Thermal-Ellipsoid Plot program for Crystal Structure Illustrations) of the molecules in the three crystal structures are shown in Figure 3 and their crystal and refinement data are listed in Table 1.

In all three cases the phenylene rings in the main conjugated chains are oriented approximately parallel to each other and the hexyl side chains are coplanar. While in **9** (Figure 3a) the alkyl side chains adopt a regular all-trans conformation, in the case of the trimers **1** and **2** they are bent (Figure 3b,c). The reasons for this behavior are intermolecular interactions as shown in Figures 4 and 5: the hexyl side chains do not interdigitate but are bent toward the main chain direction to fill the free volume between them. The average tilt angle

Table 1. Crystallographic Data of 1, 2, and 9

structure	**1**	**2**	**9**
a (Å)	5.9262(4)	5.6655(6)	8.6807(5)
b (Å)	13.897(1)	11.943(2)	9.1165(5)
c (Å)	22.503(2)	23.154(5)	23.696(2)
α (deg)	94.476(3)	84.848(6)	90
β (deg)	90.998(6)	86.150(9)	98.095(6)
γ (deg)	102.689(6)	80.216(12)	90
V (Å^3)	1801.3	1535.5	1856.5
Z	2	2	4
D_x (g cm^{-3})	1.097	1.064	1.167
μ (cm^{-1})	1.133	0.552	15.256
space group	$P\bar{1}$	$P\bar{1}$	$P2_1/n$
no. of unique reflns	7427	6061	3863
no. of observed reflns	3039	2406	2111
R	0.084	0.0583	0.0477
R_w	0.092	0.0775	0.0591
T (K)	210	210	298
λ	Mo Kα	Mo Kα	Cu Kα
diffractometer	Nonius KCCD	Nonius KCCD	Nonius CAD4

between the main chain and the side chain amounts to approximately 45° for **2** and 35° for **1**; one reason for this difference is likely to be the changed length of the molecule: **1** is longer and therefore possesses a larger volume between the backbones to be filled. Consequently, in the case of **1** the side chains can be more tilted than for **2**. According to the smaller tilt angles also, the distance between the backbones decreases from 9.5 to 9.0 Å for **2** and **1**, respectively. An important role for this decreased spacing can also be ascribed to the occurrence of hydrogen bonding between the end groups of **1** as compared to those of **2**. Similarly to the 2D case (STM image in Figure 1) the trimer molecules pack regularly parallel to each other, forming lamellar structures. Both **1** and **2** exhibit an arrangement which suggests a high conformational mobility of the side chains at room temperature. Out of six hexyl side chains, molecule **2** possesses four that are bent and two which are rather straight (Figure 3), while in molecule **1** these latter two side chains exhibit two approximately statistically occupied orientations of the last propyl function (Figure 3c).

2.4. Discussion. The spatial organization of molecules in solid states depends on intramolecular and intermolecular forces, and in 2D assemblies additionally on interfacial forces. Hence, it is of interest to compare and correlate molecular structures in single crystals and in 2D physisorbed monolayers. The phenyleneethynylene derivatives described here consist essentially of three chemical functions: the conjugated main chain, the aliphatic side chains, and the end groups (in α and ω positions). The contribution of each one in the self-assembly can be discussed. The linearity of the conjugated backbones consisting of alternating triple bonds and phenylene rings represents a geometric advantage for the generation of extremely ordered lamellae both in 2D and 3D.[8b,9] This is the case in the physisorbed 2D monolayers on HOPG where the unsaturated main chains tend to adsorb flat on the basal plane of the conductive substrate, maximizing in this way the overlap of its electronic states with the ones of the graphite, leading to a maximization of the enthalpic gain. This latter characterizes the molecular adsorption at surfaces.[8c] To adopt this 2D packing, the molecules need

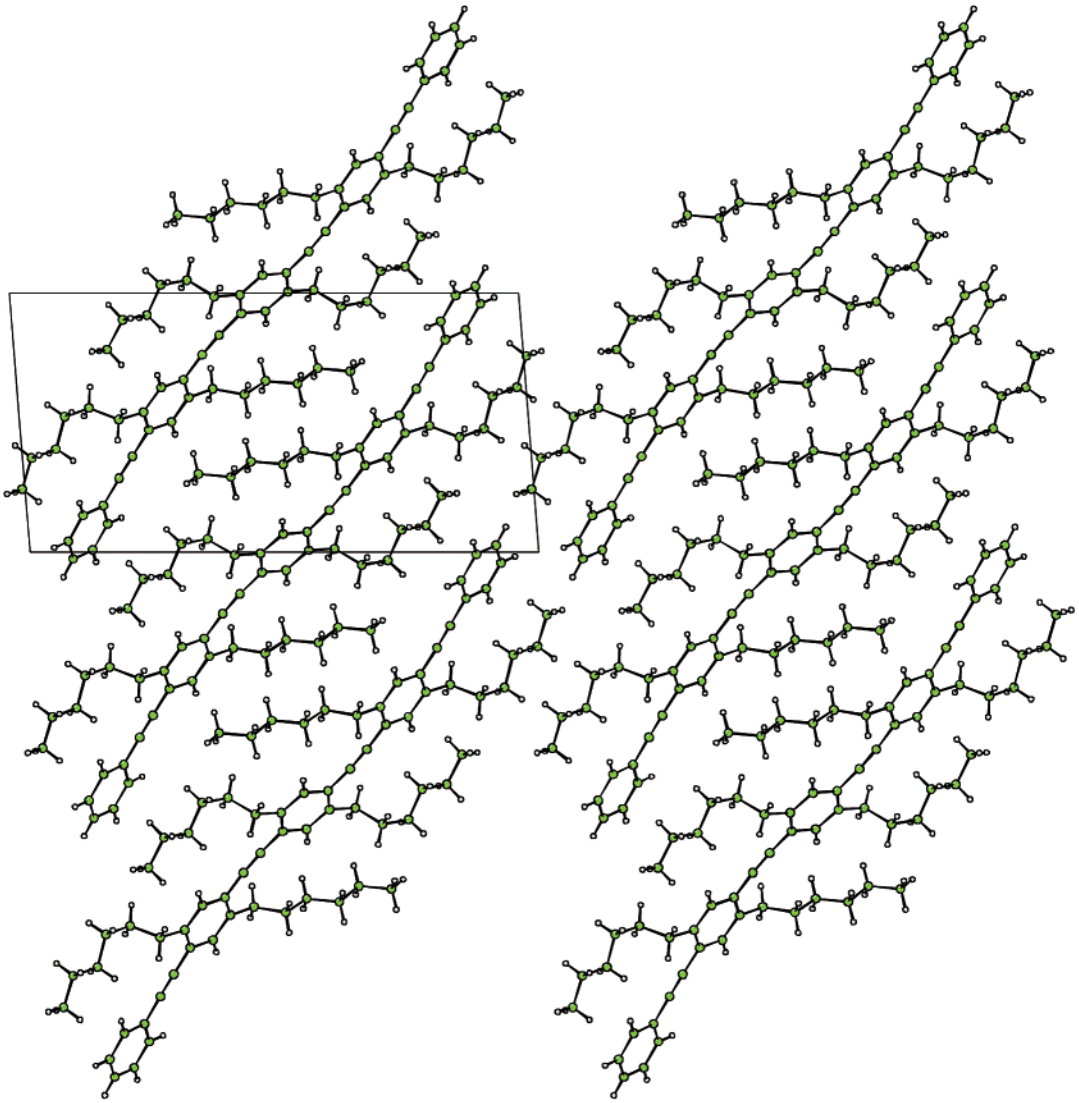

Figure 4. Crystallographic structure of **1**.

to attain a particular conformation. The required energy for this internal rearrangement can be provided by gain in adsorption energy. One rearrangement consists of the rotation of adjacent phenylene rings around the neighboring single bonds. Theoretical calculations and physical measurements have determined this barrier for diphenylacetylene, which can be regarded as a model compound of our trimer, to be less than 0.86 kcal/mol.[19] Similarly to the case of a bishexa-*peri*-hexabenzocoronenyl, this latter rotational barrier's energy is likely to be at least 1−2 orders of magnitude lower than the energy gain upon adsorption of an isolated molecule on graphite.[20] On the other hand, the lateral aliphatic chains play a prime role in conjugated oligomers and macromolecules. They are commonly attached to the backbones to enhance the solubility in organic solvents. In addition they play an important role in the self-organization of the organic system in 2D and 3D architectures on a flat solid substrate.[8,9] In the present case both XRD and STM results indicate a considerable mobility of the side chains at room temperature. In the first case, two different conformations of the terminal propyl functions of the hexyl side chains of **1** can be recognized in Figure 3c. In the latter case, with our homemade STM apparatus, which allows scanning up to about 100 Hz/line, it was not possible to resolve the structure of single hexyl chains. This can be attributed to the high conformational mobility of the relatively short alkyl chains. Indeed, the increasing order of solid-state aggregates in other PPE derivatives with an increasing length of the side chains can be in fact interpreted in terms of decreasing dynamics of the lateral substituents.[21]

Molecule **1** investigated here posseses a contour length of 4.05 nm. When thiol functionalities in α and ω position are reactivated by a simple removal of the carbamoyl protecting groups in a basic environment, the single oligomers are ready to chemisorb on two facing gold nanoelectrodes of a mechanically controllable break junction.[22] This would allow probing of the electrical properties of single molecules along their conjugated

(19) (a) Experimental measurement of the rotational barrier of tolane: Okuyama, K.; Hasegawa, T.; Ito, M.; Mikami, N. *J. Phys. Chem.* **1984**, *88*, 1711. (b) Calculation: Seminario, J. M.; Zacarias, A. G.; Tour, J. M. *J. Am. Chem. Soc.* **1998**, *120*, 3970.

(20) Ito, S.; Herwig, P. T.; Böhme, T.; Rabe, J. P.; Rettig, W.; Müllen, K. *J. Am. Chem. Soc.* **2000**, *122*, 7698.

(21) Ofer, D.; Swager, T. M.; Wrighton, M. S. *Chem. Mater.* **1995**, *7*, 418.

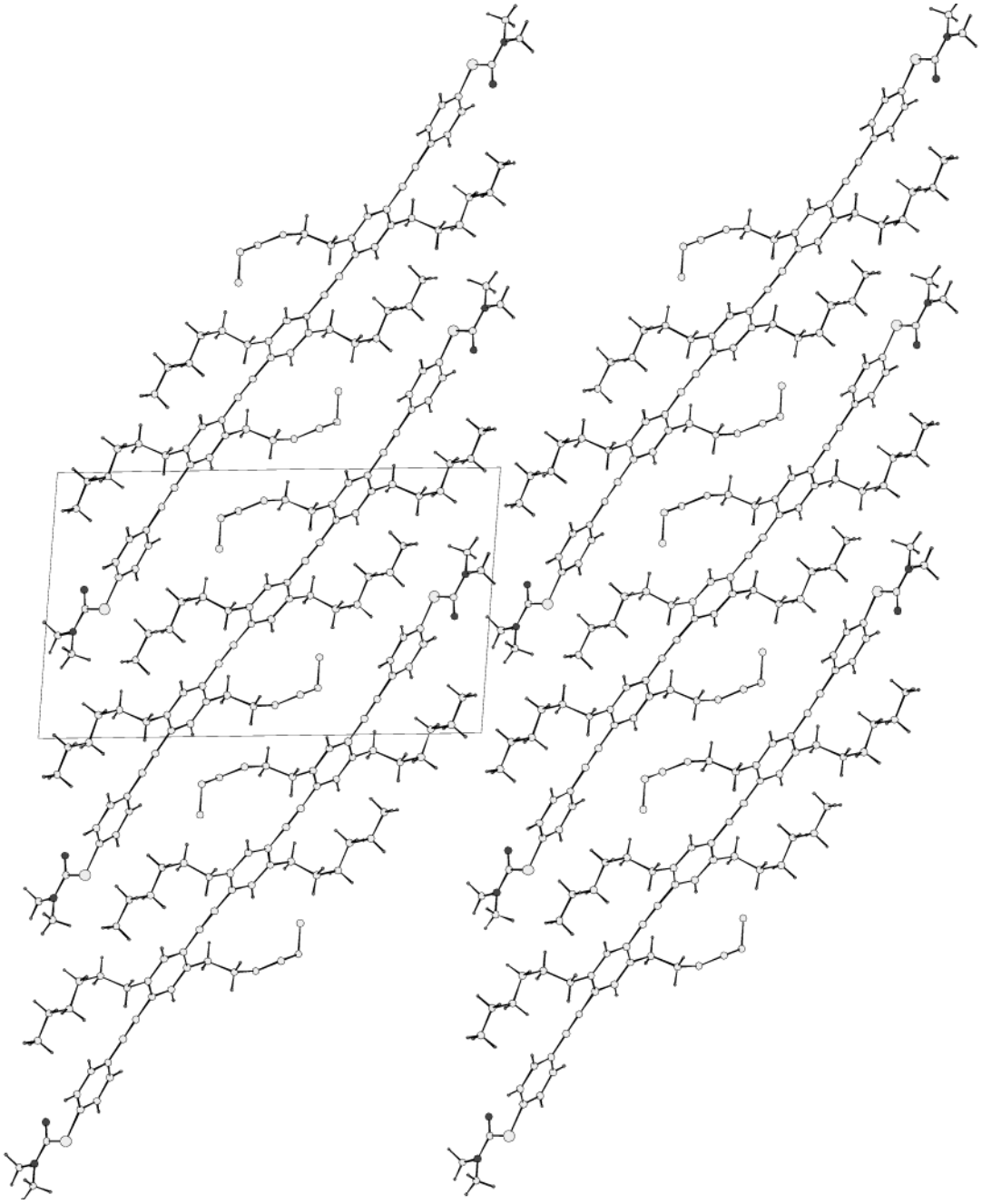

Figure 5. Crystallographic structure of **2**.

backbones in a prototype of a molecular nanowire device. In the present case these end groups interact with the neighboring molecules through the formation of hydrogen bonding, thus providing further stabilization to the molecular arrangement.[23] These types of noncovalent interactions play also a key role in inducing the conjugated skeletons to assume a staggered conformation.

3. Conclusions

In summary, single crystals and highly ordered monolayers at the interface between an organic solution and the basal plane of the graphite can be grown from end-functionalized ter-phenyleneethynylenes. The molecular arrangements that can be attained at surfaces (2D) or in solid bulk states (3D) are the result of interfacial as well as intermolecular and intramolecular forces. The distinct contributions of the different moieties composing the molecule in the self-assembly into the supramolecular structures have been discussed. Both these two "hairy rod" oligomers have shown a high stiffness along the backbone, while the hexyl side chains possess a high conformational mobility at room tem-

(22) Reed, M. A.; Zhou, C.; Muller, C. J.; Burgin, T. P.; Tour, J. M. *Science* **1997**, *278*, 252.

(23) (a) Desiraju, G. R. *Acc. Chem. Res.* **1996**, *29*, 441. (b) Hirschberg, J. H. K. K.; Brunsveld, L.; Ramzi, A.; Vekemans, J. A. J. M.; Sijbesma, R. P.; Meijer, E. W. *Nature* **2000**, *407*, 167. (c) Gottarelli, G.; Masiero, S.; Mezzina, E.; Pieraccini, S.; Rabe, J. P.; Samorí, P.; Spada, G. P. *Chem. Eur. J.* **2000**, *6*, 3242. (d) Barth, J. V.; Weckesser, J.; Cai, C.; Günter, P.; Bürgi, L.; Jeandupeux, O.; Kern, K. *Angew. Chem., Int. Ed.* **2000**, *39*, 1230. *Angew. Chem.* **2000**, *112*, 1285. (e) Yabuuchi, K.; Rowan, A. E.; Nolte, R. J. M.; Kato, T. *Chem. Mater.* **2000**, *12*, 440. (f) Raymo, F. M.; Bartberger, M. D.; Houk, K. N.; Stoddart, J. F. *J. Am. Chem. Soc.* **2001**, *123*, 9264.

perature. The molecular ordering in these two architectures appears different: the different contour lengths of the molecules along the main chain induce the aliphatic side groups to adopt a different tilt angle with respect to the conjugated skeleton, leading to a different interchain distance. This could be interesting for tuning the interchain hopping. Finally, the possibility of controlling the molecular aggregation is of importance in the development of molecular electronic devices such as molecular nanowires, light-emitting diodes, and solid-state lasers.

Experimental Section

Techniques. Scanning tunneling microscopy investigations have been employed at the interface between an almost saturated solution and the basal plane of the freshly cleaved highly oriented pyrolitic graphite substrate (HOPG, grade ZYB, Advanced Ceramics, Cleveland, OH). The solutions have been prepared desolving the crystalline powder of **1** in 1-phenyloctane (Aldrich).

Tunneling tips were electrochemically etched (KOH, 2N + NaCN, 6N) or mechanically cut from a 0.25-mm Pt/Ir (80:20) wire. The physisorbed films were studied with a homemade low current-beetle type scanning tunneling microscope running with Omicron electronics.[24] Typical scan rates were 50−200 Hz/line for imaging on a sub-nanometer scale (constant height mode). Changing the tunneling parameters, we were able to visualize both the structure of the HOPG and the adsorbed monolayer. This enabled us to calibrate the scanner while measuring. The dimensions of the unit cell of the adsorbate were evaluated by SPIP software.[25]

Single crystals of either **1** or **2** were prepared by mixing respectively **1** or **2** first with boiling ethyl acetate and then with petroleum until complete dissolution. The concentrated solution was cooled from 80 °C to room temperature within 3 days to yield pale yellow needle-shaped single crystals, which are suitable for XRD.

XRD investigations have been executed on the single crystals. Compound **9** has been studied with a Nonius CAD4 diffractometer with graphite monochromated Cu Kα radiation while **1** and **2** have been analyzed using a Nonius Kappa-CCD apparatus with graphite monocromated Mo Kα radiation. Pertinent crystallographic data and details of the structure refinements are summarized in Table 1. The structures were solved by direct methods (SIR92) and refined by full-matrix least-squares analyses. All non-hydrogen atoms except for the disordered C atoms in one of the side chains were refined with anisotropic temperature factors. The latter were refined with isotropic temperature factors and the occupancy factor was included in the refinement. The hydrogen atoms were refined in the riding mode with fixed isotropic temperature factors.

The contour lengths of the trimers have been evaluated using a molecular modeling package DISCOVER VERSION 4.0.0, Biosym Technologies Inc., San Diego, CA.

All starting materials were obtained from commercial suppliers and used without further purification. The reaction apparatus was predried and the reactions were carried out under an argon atmosphere. Triethylamine was distilled over KOH before use. THF was distilled over potassium and kept under argon. ^{1}H and ^{13}C NMR chemical shifts were obtained using Varian Gemini 200, Bruker AMX 300, and Bruker AMX 500 spectrometers and expressed in parts per million (δ) with residual H atoms in the deuterated solvent as the internal standard. Mass spectra were obtained using a VG Instruments ZAB2-SE-FPD (FD). IR were recorded using a Nicolet FT-IR 320. The UV−vis absorption spectra were measured with a Perkin-Elmer Lambda 9.

(24) Hillner, P. E.; Wolf, J. F.; Rabe, J. P., Humboldt University Berlin, unpublished.

(25) *SPIP Scanning Probe Image Processor, Version 1.73*; Image Metrology ApS: Lyngby, Denmark.

1,4-Bis[[2,5-dihexyl-4-(trimethylsilylethynyl)phenyl]-ethynyl]-2,5-dihexylbenzene (5). To a solution of 2,5-dihexyl-4-[(trimethylsilyl)ethynyl]iodobenzene (**3**) (5.54 g, 11.89 mmol) and 1,4-diethynyl-2,5 dihexylbenzene (**4**) (1.70 g, 5.78 mmol) in 7 mL of triethylamine and 80 mL of tetrahydrofuran were added $Pd(PPh_3)_4$ (62 mg, 0.06 mmol, 0.5 mol %), CuI (23 mg, 0.12 mmol, 1.0 mol %), and triphenylphosphine (31 mg, 0.12 mmol, 1.0 mol %). The mixture was stirred at 80 °C for 24 h. After removal of the solvent in vacuo, the crude material was purified by column chromatography using silica gel with light petroleum as eluent to yield 4.72 g (4.83 mmol, 82%.) of a pale yellow product; mp 95 °C. ^{1}H NMR (300 MHz, chloroform-*d*, 30 °C): δ_H 7.33 (s, 2 H), 7.29 (s, 2 H), 7.28 (s, 2 H), 2.85−2.64 (m, 12 H, hexyl), 1.76−1.50 (m, 12 H, hexyl), 1.45−1.21 (m, 36 H, hexyl), 0.95−0.79 (m, 18 H, hexyl), 0.25 (18 H, TMS). ^{13}C NMR (75 MHz, chloroform-*d*, 30 °C): δ_C 142.8, 141.9, 141.8, 132.5, 132.4, 123.0, 122.8, 122.4, 104.1, 99.0, 93.0 (C≡C), 34.2, 31.8, 31.7, 30.7, 29.3, 22.6, 14.1 (hexyl), 0.1 (TMS). IR (KBr): $\tilde{\nu}$ [cm^{-1}] 3025 (w), 2956 (s), 2924 (s), 2854 (s), 2361 (m), 2335 (m), 2149 (m) [C≡C], 1603 (w), 1497 (m), 1461 (m), 1407 (m), 1375 (m), 1249 (s), 1220 (m), 1178 (w), 1118 (w), 1070 (w), 894 (m) 855 (s), 844 (s), 759 (m), 649 (m). UV/vis (chloroform): λ [nm] (log ϵ [l mol^{-1} cm^{-1}]) 317 (3.56), 355 (3.90), 377 (3.78), 401 (3.08). MS (FD): m/z [u e^{-1}] = 487 (M^{2+}), 975 (M^+), 1951 (2 M^+). Anal. Calcd: C, 83.71; H, 10.54; Si, 5.76. Found: C, 83.79; H, 10.48.

1,4-Bis[(4-ethynyl-2,5-dihexylphenyl)ethynyl]-2,5-dihexylbenzene (6). 1,4-Bis[[2,5-dihexyl-4-(trimethylsilylethynyl)phenyl]ethynyl]-2,5-dihexylbenzene (**5**) (4.00, 4.10 mmol) was dissolved in 30 mL of diethyl ether. To the solution was added KOH (1.15 g, 20.51 mmol) dissolved in 5 mL of methanol and the mixture was stirred under exclusion of oxygen and light at room temperature for 14 h. After the addition of 30 mL of dichloromethane, the organic phases were washed with distilled water three times and then dried with $MgSO_4$. The solvent was removed in vacuo and the crude material was purified by chromatography using a short column of silica gel and light petroleum as eluent to yield 3.31 g (97%) of a pale yellow product; mp 102 °C (decomposition). ^{1}H NMR (500 MHz, chloroform-*d*, 30 °C): δ_H 7.39−7.31 (m, 6 H), 3.28 (s, 2 H, C≡C−H), 2.91−2.70 (m, 12 H, hexyl), 1.81−1.62 (m, 12 H, hexyl), 1.48−1.21 (m, 36 H, hexyl), 0.97−0.79 (m, 18 H, hexyl). ^{13}C NMR (50 MHz, tetrachlorethane-d_2, 30 °C): δ_C 143.3, 142.4, 142.3, 133.4, 132.8, 132.5, 132.3, 129.3, 129.1, 123.7, 123.2, 121.8, 93.6, 93.3 (C≡C), 83.0, 82.4 (C≡C−H), 34.5, 34.3, 32.2, 32.1, 31.0, 30.9, 29.7, 29.6, 23.1, 14.6 (hexyl). UV/vis (chloroform): λ [nm] (log ϵ [l mol^{-1} cm^{-1}]) 323 (3.37), 395 (3.89). MS (FD): m/z [u e^{-1}] 415.5 (M^{2+}), 831.0 (M^+). Anal. Calcd: C, 89.57; H, 10.43. Found: C, 83.93; H, 10.65.

1,4-Bis[[2,5-dihexyl-4-[[4-[(*N*,*N*-dimethylcarbamoyl)-thio]phenyl]ethynyl]phenyl]ethynyl]2,5-dihexylbenzene (1). 1,4-Bis[(4-ethynyl-2,5-dihexylphenyl)ethynyl]-2,5-dihexylbenzene (**6**) (2.80 g, 3.37 mmol) and 4-[(*N*,*N*-dimethylcarbamoyl)thio]iodobenzene (**7**) (2.59 g, 8.42 mmol) were dissolved in 3 mL of triethylamine and 50 mL of tetrahydrofuran. The resulting solution was degassed three times by applying vacuum, and then $Pd(PPh_3)_4$ (195 mg, 0.17 mmol, 5.0 mol %) and CuI (64 mg, 0.34 mmol, 10.0 mol %) were added. The mixture was heated and stirred for 24 h at 60 °C. The solvent was evaporated and the residue was dissolved in as little dichloromethane as possible and precipitated in 200 mL of methanol to remove the excess of **7**. The crude material was purified by column chromatography using silica gel with light petroleum/ethyl acetate (3:1) as eluent to yield 2.46 g (2.07 mmol, 73%) of a pale yellow product, mp: 136 °C. ^{1}H NMR (500 MHz, chloroform-*d*, 30 °C): δ_H 7.51 (dd, ^3J = 8.5 Hz, ^4J = 2.1 Hz, 4 H, end group), 7.47 (dd, ^3J = 8.5 Hz, ^4J = 2.1 Hz, 4 H, end group), 7.37−7.34 (m, 6 H), 3.06 (s, 12 H, $N(CH_3)_2$), 2.85−2.76 (m, 12 H, hexyl), 1.76−1.64 (m, 12 H, hexyl), 1.47−1.23 (m, 12 H, hexyl), 0.93−0.82 (m, 18 H, hexyl). ^{13}C NMR (125 MHz, chloroform-*d*, 30 °C): δ_C 166.3 (C=O), 142.4, 141.9, 135.5, 132.5, 132.4, 132.3, 131.7, 129.0, 124.4, 123.0, 122.8, 122.3, 93.4, 93.1, 93.1, 89.9 (C≡C), 36.9 ($N(CH_3)_2$), 34.2, 34.2, 34.2, 31.8, 31.8, 30.7, 30.7, 29.3, 22.6, 22.6, 14.1 (hexyl). IR (KBr): $\tilde{\nu}$ [cm^{-1}] 2955 (s), 2921 (s), 2851 (s), 1725 (w), 1675 (m)

[C═O], 1590 (w), 1503 (w), 1460 (m), 1376 (m), 1267 (w), 1216 (m), 1101 (m), 1088 (m), 1020 (w), 970 (w), 903 (w), 830 (w), 799 (s), 686 (m). UV/Vis (chloroform): λ [nm] (log ϵ [l mol^{-1} cm^{-1}]) 323 (3.92), 368 (4.31). MS (FD): *m*/*z* [u e^{-1}] 595 (M^{2+}), 1190 (M^{+}). Anal. Calcd: C, 80.76; H, 8.81; N, 2.35; S, 5.39. Found: C, 80.86; H, 8.92; N, 2.15; S, 5.26.

α-Phenylethynyl-ω-phenyl-ter[(2,5-dihexylphenylene-1,4)ethynylene)] (2). 1,4-Bis[(4-ethynyl-2,5-dihexylphenyl)-ethynyl]-2,5-dihexylbenzene (**6**) (1.30 g, 1.56 mmol) and iodobenzene (**8**) (0.96 g, 4.69 mmol) were dissolved in 3 mL of triethylamine and 40 mL of tetrahydrofuran. The resulting solution was degassed three times with vacuum, and then Pd(PPh$_3$)$_4$ (90 mg, 0.08 mmol, 5.0 mol %) and CuI (30 mg, 0.16 mmol, 10.0 mol %) were added. The mixture was heated and stirred for 24 h at 60 °C. The solvent was evaporated and the crude material was purified by column chromatography using silica gel with light petroleum/ethyl acetate (9.5:0.5) as eluent to yield 1.25 g (1.27 mmol, 81%) of a pale yellow product, mp: 94 °C. ^{1}H NMR (500 MHz, chloroform-*d*, 30 °C): δ_H 7.53 (dd, ^3J = 7.9 Hz, ^4J = 1.5 Hz, 4 H, end group), 7.39−7.32 (m, 6 H, end group, 6 H, remaining aromatic protons), 2.87−2.78 (m, 12 H, hexyl), 1.77−1.66 (m, 12 H, hexyl), 1.48−1.27 (m, 36 H, hexyl), 0.95−0.82 (m, 18 H, hexyl). ^{13}C NMR (125 MHz, chloroform-*d*, 30 °C): δ_C 142.3, 141.9, 132.5, 132.3, 131.5, 128.4, 128.2, 123.6, 122.8, 122.6, 94.0, 93.1, 93.0, 88.5 (C≡C), 34.2, 31.8, 31.8, 30.7, 30.7, 29.3, 29.3, 22.7, 22.6, 14.1 (hexyl). IR (KBr): $\tilde{\nu}$ [cm^{-1}] 2953 (s), 2927 (s), 2868 (s), 1663 (m) [C═O], 1591 (w), 1501 (w), 1476 (m), 1398 (w), 1361 (m), 1258 (w), 1101 (m), 1086 (m), 1058 (w), 1016 (w), 905 (w), 826 (w), 686 (m). FD: *m*/*z* [u e^{-1}] 635 (100%, M^{+}). Anal. Calcd: C, 90.37; H, 9.63. Found: C, 90.33; H, 9.71.

1,4-Bis[2-[4-[(*N*,*N*-dimethylcarbamoyl)thio]phenyl]-ethynyl-2,5-dihexylbenzene (9). To a solution of 1,4-diethynyl-2,5-dihexylbenzene (**4**) (1.00 g, 3.40 mmol) and 4-[(*N*,*N*-dimethylcarbamoyl)thio]iodobenzene (**7**) (2.30 g, 7.48 mmol) in 20 mL of triethylamine and 30 mL of tetrahydrofuran were added Pd(PPh$_3$)$_4$ (173 mg, 0.15 mmol, 2.0 mol %) and CuI (57 mg, 0.30 mmol, 4.0 mol %). The mixture was stirred at 60 °C for 24 h. After addition of 80 mL of water, the aqueous phase was extracted with CH_2Cl_2. The combined organic layers were washed with water three times and then dried with $MgSO_4$. After removal of the solvent in vacuo, the crude material was purified by column chromatography using silica gel with dichloromethane as eluent. The product was recrystallized from methanol and dried in vacuo to yield 31.8 g (1.53 g, 2.41 mmol, 71%) of colorless needles; mp: 76 °C.

^{1}H NMR (250 MHz, chloroform-*d*, 30 °C): δ_H 7.48 (m, 8 H, end group), 7.34 (s, 2 H), 3.05 (m, 12 H), 2.77 (t, 4 H, hexyl), 1.66 (q, 4 H, hexyl), 1.40−1.36 (m, 4 H, hexyl), 1.32−1.29 (m, 8 H), 0.86 (t, 6 H, hexyl). ^{13}C NMR (62 MHz, chloroform-*d*, 30 °C): δ_C 166.1 (C═O), 142.3, 135.3, 132.3, 131.6, 129.1, 122.4, 122.2, 93.5, 89.8 (C≡C), 36.8, 34.1, 31.6, 30.5, 29.1, 22.5, 14.0 (hexyl). IR (KBr): $\tilde{\nu}$ [cm^{-1}] 3016 (w), 2955 (s), 2921 (s), 2854 (s), 1725 (w), 1593 (w), 1538 (m), 1502 (m), 1453 (m), 1378 (m), 1215 (s), 1065 (w), 971 (w), 899 (w), 756 (s), 689 (m), 668 (m). UV/vis (chloroform): λ [nm] (log ϵ [l mol^{-1} cm^{-1}]) 282 (3.65), 321 (3.82), 364 (4.17), 384 (4.04). FD: *m*/*z* [u e^{-1}] 492 (8%, M^{2+}), 983 (100%, M^{+}). Anal. Calcd: C, 73.58; H, 7.42; N, 4.29; S, 9.80. Found: C, 7.57; H, 7.57; N, 4.19; S, 9.86.

Acknowledgment. This work was supported by TMR project SISITOMAS, the Volkswagen-Stiftung (Elektronentransport durch konjugierte molekulare Scheiben und Ketten), the European Science Foundation through SMARTON, and the German "Bundesministerium fuer Forschung und Technologie" as part of the program "Zentrum fuer multifunktionelle Werkstoffe und miniaturisierte Funktionseinheiten". P.S. wishes to thank the EU for a TMR grant.

CM0212459